

Short communication

Investigations on electrical conductivity and chemical compatibility between fast lithium ion conducting garnet-like $\text{Li}_6\text{BaLa}_2\text{Ta}_2\text{O}_{12}$ and lithium battery cathodes

V. Thangadurai*, W. Weppner

Chair for Sensors and Solid State Ionics, Faculty of Engineering, University of Kiel, Kaiserstr. 2, D-24143 Kiel, Germany

Received 13 August 2004; received in revised form 25 October 2004; accepted 2 November 2004

Available online 21 December 2004

Abstract

Garnet-like metal oxide with the nominal chemical composition $\text{Li}_6\text{BaLa}_2\text{Ta}_2\text{O}_{12}$ was prepared by conventional solid-state reaction method. It shows mainly bulk contribution to the total lithium ion conductivity. The thick and thin $\text{Li}_6\text{BaLa}_2\text{Ta}_2\text{O}_{12}$ pellets exhibit similar lithium ion conductivity over the investigated temperature range (RT–370 °C). The chemical compatibility between garnet-like $\text{Li}_6\text{BaLa}_2\text{Ta}_2\text{O}_{12}$ and several potential lithium battery positive (cathode) electrodes that includes LiCoO_2 , LiNiO_2 , LiMn_2O_4 and $\text{Li}_2\text{MMn}_3\text{O}_8$ (M = Fe, Co) was investigated by powder X-ray diffraction (XRD). 1:1 wt.% $\text{Li}_6\text{BaLa}_2\text{Ta}_2\text{O}_{12}$ and electrode powders were mixed and heated in the temperature range 400–900 °C for 24 h in air. The powder XRD data reveals that $\text{Li}_6\text{BaLa}_2\text{Ta}_2\text{O}_{12}$ is stable against chemical reaction with layered structure LiCoO_2 over the investigated temperature range, while the Mn, (Co, Mn), (Fe, Mn) and Ni containing electrodes were found to react above 400 °C. Accordingly, LiCoO_2 electrode may be considered as potential positive electrode with $\text{Li}_6\text{BaLa}_2\text{Ta}_2\text{O}_{12}$ electrolyte for galvanic cell applications (e.g., batteries).

© 2004 Elsevier B.V. All rights reserved.

Keywords: Solid-state lithium ion conductors (SSLICs); $\text{Li}_6\text{BaLa}_2\text{Ta}_2\text{O}_{12}$; Pseudo-garnets; Chemical compatibility; AC impedance; Electrical properties

1. Introduction

Development of practically useful ceramic solid-state lithium ion conductors (SSLICs) for high performance all-solid-state lithium batteries and other galvanic cell applications is an ongoing task and drawn much interest in recent years [1,2]. Lithium batteries are an attractive energy source for portable electronic equipments (e.g., notebooks, cameras, toys, mobile phones, etc.) and transport applications. In order to employ the SSLIC in the high energy density lithium secondary batteries, it should have following desired electrical and physical properties:

- (i) High lithium ion conductivity at operating temperature (preferably at room temperature).

- (ii) Negligible electronic conductivity over the entire employed range of lithium activity and temperature.
- (iii) Negligibly small/or no grain-boundary resistance.
- (iv) Stability against chemical reaction with both electrodes, especially with elemental Li or Li-alloy negative electrode during the preparation and operation of the cell and thermal expansion coefficient (TEC) that matches with the electrodes (cathode and anode).
- (v) High electrochemical decomposition voltage (higher than 5.5 V versus Li).
- (vi) Environmental benignity, non-hygroscopic, low cost and easiness of preparation.

Several crystalline and/or amorphous (glass) inorganic oxide and non-oxide compounds exhibit fast lithium ion conduction [1,2]. However, silicate (SiO_4^{4-}) and phosphate (PO_4^{3-}) frame-work structure based electrolytes are being employed as electrolyte in the all-solid-state batteries due to

* Corresponding author. Tel.: +49 431 880 6210; fax: +49 431 880 6203.
E-mail address: vt@tf.uni-kiel.de (V. Thangadurai).

their high electrochemical stability and chemical compatibility with both electrodes (cathode and anode) [3].

Novel garnet-type lithium containing transition metal oxides [4,5] with the nominal chemical compositions $\text{Li}_5\text{La}_3\text{M}_2\text{O}_{12}$ ($\text{M}=\text{Nb}, \text{Ta}$) and $\text{Li}_6\text{ALa}_2\text{M}_2\text{O}_{12}$ ($\text{A}=\text{Ca}, \text{Sr}, \text{Ba}$; $\text{M}=\text{Nb}, \text{Ta}$) were found to exhibit fast lithium ion conductivity [6–10]. AC impedance study reveals that both the Sr- and Ba-substituted $\text{Li}_5\text{La}_3\text{M}_2\text{O}_{12}$ compounds show mainly bulk contribution with a rather small (~ 10 – 14%) grain-boundary contribution at room temperature, compared to that of the corresponding parent compounds [8,9]. The grain-boundary contribution decreases with increase in temperature. Among the materials investigated, $\text{Li}_6\text{BaLa}_2\text{Ta}_2\text{O}_{12}$ exhibits the highest lithium ion conductivity of $4 \times 10^{-5} \text{ S cm}^{-1}$ at 22°C with an activation energy (E_a) of 0.40 eV [9]. The room temperature conductivity value is comparable to other fast lithium ion conductors, especially with the presently employed thin film solid electrolyte lithium phosphorus oxynitride (lipon) ($\sigma = 3.3 \times 10^{-6} \text{ S cm}^{-1}$ at 25°C ; $E_a = 0.54 \text{ eV}$) for all-solid-state lithium batteries [3].

It was observed that $\text{Li}_6\text{ALa}_2\text{Ta}_2\text{O}_{12}$ ($\text{A}=\text{Sr}, \text{Ba}$) show a single semicircle using elemental lithium reversible electrodes with a total resistance of $22.5 \text{ k}\Omega$ for the Sr- and $7.5 \text{ k}\Omega$ for the Ba-substituted compound at 23°C , respectively. A similar resistance values were obtained by DC method. The above result suggests that the absence of electrolyte–electrode interface resistance. Furthermore, the DC electrical measurements reveal that the electronic conductivity is much small and exhibit high electrochemical stability of about 6 V against metallic lithium at room temperature [9,10].

In the present study, we report the studies on electrical conductivity properties of $\text{Li}_6\text{BaLa}_2\text{Ta}_2\text{O}_{12}$ pellets having two different thicknesses by AC impedance method. As expected, both the thick and thin $\text{Li}_6\text{BaLa}_2\text{Ta}_2\text{O}_{12}$ pellets exhibit similar lithium ion conductivity, which is consistent with the literature data. Chemical compatibility between $\text{Li}_6\text{BaLa}_2\text{Ta}_2\text{O}_{12}$ and lithium battery positive electrode materials such as LiCoO_2 , $\text{Li}_2\text{MMn}_3\text{O}_8$ ($\text{M}=\text{Fe}, \text{Co}$), LiNiO_2 and LiMn_2O_4 was investigated in air using powder X-ray diffraction (XRD). Our results show that $\text{Li}_6\text{BaLa}_2\text{Ta}_2\text{O}_{12}$ have good chemical stability against reaction with layered structure LiCoO_2 up to 900°C , while the Mn, (Fe, Mn), (Co, Mn) and Ni containing electrodes were found to react at above 400°C .

2. Experimental aspects

2.1. Synthesis and phase characterization

Compounds of the nominal chemical composition $\text{Li}_6\text{BaLa}_2\text{Ta}_2\text{O}_{12}$ was prepared by solid-state reaction using stoichiometric amounts of high purity ($>99.9\%$) La_2O_3 (pre-dried at 900°C for 24 h), $\text{LiOH}\cdot\text{H}_2\text{O}$ (about 10 wt.% excess was added to compensate for the loss of lithium at

elevated temperatures), $\text{Ba}(\text{NO}_3)_2$ and Ta_2O_5 . The mixtures were heated in air and kept at 700°C for 6 h and then annealed at 900°C for 24 h. Before and after the first step, the powders were ball-milled using zirconia balls for over night in 2-propanol. For the second step of heat treatment, the reaction products were pressed into pellets by isostatic pressure and covered with powder of the same mother composition to reduce the possible loss of lithium due to volatilization. Powder X-ray diffraction (XRD) (SEIFERT 3000, $\text{Cu K}\alpha$) was employed at room temperature to monitor the phase formation after each annealing step.

2.2. Electrical characterization

Electrical conductivity measurements in ambient atmosphere on two different $\text{Li}_6\text{BaLa}_2\text{Ta}_2\text{O}_{12}$ pellets having varying thickness (sample # 1: 1.3 mm thickness, 8.3 mm diameter; sample # 2: 11.74 mm thickness, 9.24 mm diameter) were made by using lithium ion blocking Au-electrodes (Au-paste painted on parallel surfaces and cured at 700°C for 1 h to form an electrode) in the temperature range from RT to 370°C by employing an HP4192 an impedance and gain-phase analyzer (5–13 MHz). A two-probe cell was used for these measurements. Prior to each impedance measurement, the sample was equilibrated for a few hours at constant temperature. The measurements were made during the heating and cooling runs.

2.3. Chemical reactivity between $\text{Li}_6\text{BaLa}_2\text{Ta}_2\text{O}_{12}$ and lithium battery cathode materials

Chemical reaction stability of $\text{Li}_6\text{BaLa}_2\text{Ta}_2\text{O}_{12}$ with several potential lithium battery cathode materials was investigated by reacting 1:1 wt.% of mixed powders at $400, 600, 800$ and 900°C for 24 h in air. Commercially available (Merck, Darmstadt, Germany) LiCoO_2 , LiNiO_2 , and LiMn_2O_4 cathode powders were mixed with $\text{Li}_6\text{BaLa}_2\text{Ta}_2\text{O}_{12}$ powders and ball milled for over-night in 2-propanol. The powders of $\text{Li}_2\text{MMn}_3\text{O}_8$ ($\text{M}=\text{Fe}, \text{Co}$) were prepared by glycine-nitrate combustion method. Appropriate amounts of LiNO_3 , $\text{Co}(\text{NO}_3)_3\cdot 6\text{H}_2\text{O}$, $\text{Fe}(\text{NO}_3)_3\cdot 9\text{H}_2\text{O}$, $\text{Mn}(\text{NO}_3)_2\cdot 4\text{H}_2\text{O}$ and $\text{H}_2\text{NCH}_2\text{CO}_2\text{H}$ were dissolved in a minimum volume of deionized water to obtain aqueous solution. These solutions were heated to 300°C to obtain powders. After the combustion, the powders were heated at 700°C for 2 h in air [11]. The resultant product shows the formation of spinel-type structure and is consistent with the literature data [12,13].

3. Results and discussion

3.1. Structure and lithium ion conductivity

Powder XRD data shows the formation of garnet-like structured $\text{Li}_6\text{BaLa}_2\text{Ta}_2\text{O}_{12}$. Typical impedance plot obtained at 30°C for $\text{Li}_6\text{BaLa}_2\text{Ta}_2\text{O}_{12}$ pellets (samples # 1 and

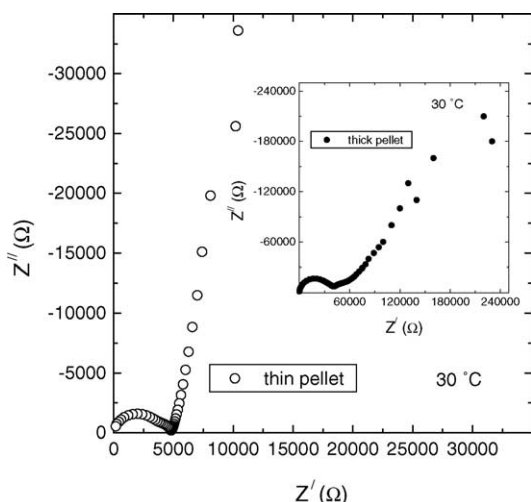


Fig. 1. Typical impedance plot obtained for $\text{Li}_6\text{BaLa}_2\text{Ta}_2\text{O}_{12}$ in air at $30\text{ }^\circ\text{C}$ using Au electrodes of thin pellet (1.3 mm height; 8.3 mm diameter) in the frequency range 5 Hz–13 MHz. The insert shows the corresponding data of thick pellet (11.74 mm height; 9.24 mm diameter). We see a major bulk-contribution at the high-frequency side and small grain-boundary contribution and spike at low frequency regime. The appearance of a tail at the low frequency side suggests a blocking of the electrode for the mobile lithium ions.

2) are shown in Fig. 1. In both cases, we see a large bulk contribution at high frequency side, small grain-boundary and a spike at low frequency regime. The results are consistent with our previous investigation [8,9]. The appearance of a tail at the low frequency side suggests a blocking of the electrode for the mobile lithium ions [14,15]. The low temperature impedance plots could be well resolved into bulk, grain-boundary and electrode effects. The grain-boundary contribution decreases with increasing temperature and difficult to separate at high temperature regime. For experimental and practical applications, we have considered the total (bulk + grain-boundary) contribution for the determination of lithium ion conductivity.

Fig. 2 shows the Arrhenius plots for the lithium ion conductivity of samples # 1 (thin pellet) and # 2 (thick pellet). The data obtained from the first heating and cooling runs follow the same line suggesting equilibrium conductivity behaviour. As expected, both thin and thick pellets show similar electrical conductivities. The activation energy for electrical conductivity was found to be 0.40 eV. In Fig. 3, we give the room temperature conductivity of $\text{Li}_6\text{BaLa}_2\text{Ta}_2\text{O}_{12}$ as a function of time. The data shows that there is no significant ageing effect over the investigated period of 15 days; however, a very small variation in the electrical conductivity was observed.

3.2. Chemical compatibility

Several lithium containing transition metal oxides LiCoO_2 , LiNiO_2 , LiMn_2O_4 and $\text{Li}_2\text{MMn}_3\text{O}_8$ ($M = \text{Fe}, \text{Co}$) are well-known as positive electrode (cathode) materials for the lithium ion secondary batteries [16]. Among them, 2D

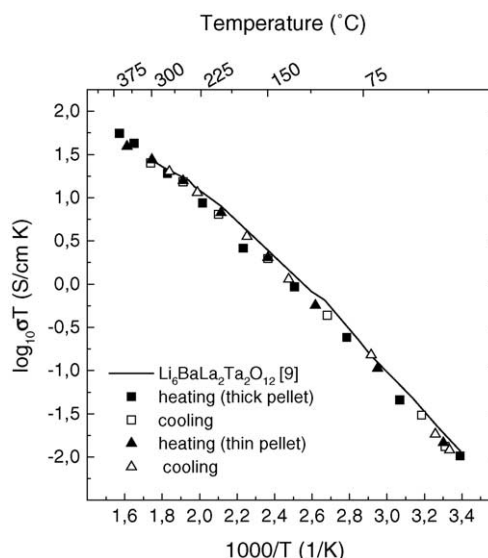


Fig. 2. The Arrhenius plots for electrical conductivity of $\text{Li}_6\text{BaLa}_2\text{Ta}_2\text{O}_{12}$ measured using lithium ion blocking Au electrodes of thin pellet (8.3 mm diameter; 1.3 mm height) and thick pellet (9.24 mm diameter; 11.74 mm height). For comparison, the data from literature is included [9]. We see that both thick and thin samples show a similar conductivity data and consistent with the literature value, indicating an excellent reproducibility.

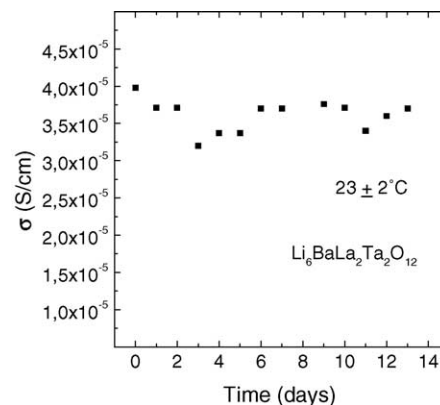


Fig. 3. The electrical conductivity data of $\text{Li}_6\text{BaLa}_2\text{Ta}_2\text{O}_{12}$ as a function of time at room temperature.

layered structure LiCoO_2 is being employed in the commercial production of polymer electrolyte based lithium ion secondary batteries [17], due to its good reversible lithium intercalation and deintercalation reactions. Recently, LiCoO_2 and LiMn_2O_4 cathodes have been considered for the development of thin film all-solid-state lithium secondary batteries using thin film LiPON as a solid electrolyte [3]. Accordingly, we have selected above cathode materials for the compatibility investigation with garnet-type electrolyte $\text{Li}_6\text{BaLa}_2\text{Ta}_2\text{O}_{12}$, to screen suitable electrodes for galvanic cell applications.

Figs. 4–7 show the powder XRD patterns of $\text{Li}_6\text{BaLa}_2\text{Ta}_2\text{O}_{12}$ and electrode (LiCoO_2 , LiMn_2O_4 , LiNiO_2 and $\text{Li}_2\text{CoMn}_3\text{O}_8$) mixtures heated at 400, 600, 800 and 900 $^\circ\text{C}$ for 24 h in air. Surprisingly, we see only diffraction peaks due to garnet-like structure $\text{Li}_6\text{BaLa}_2\text{Ta}_2\text{O}_{12}$ and layered

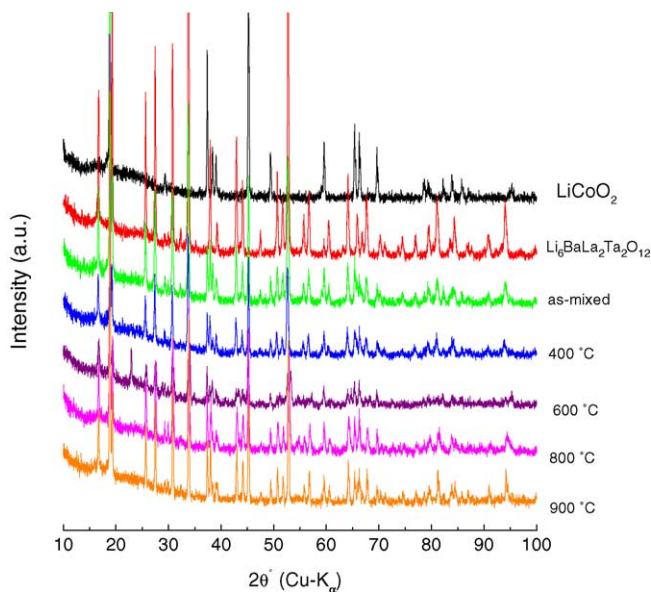


Fig. 4. Powder XRD patterns showing the reactivity between $\text{Li}_6\text{BaLa}_2\text{Ta}_2\text{O}_{12}$ and LiCoO_2 mixture at 400, 600, 800 and 900 °C in air. We see only the reflections due to garnet-like $\text{Li}_6\text{BaLa}_2\text{Ta}_2\text{O}_{12}$ and layered structure LiCoO_2 in the reaction products. The results suggest that $\text{Li}_6\text{BaLa}_2\text{Ta}_2\text{O}_{12}$ is chemically stable against reaction with LiCoO_2 .

structure LiCoO_2 in the powder XRD patterns (Fig. 4) in the reaction products of $\text{Li}_6\text{BaLa}_2\text{Ta}_2\text{O}_{12}$ and LiCoO_2 mixtures. The result suggests that no significant chemical reaction occurred between $\text{Li}_6\text{BaLa}_2\text{Ta}_2\text{O}_{12}$ and LiCoO_2 under the investigated condition.

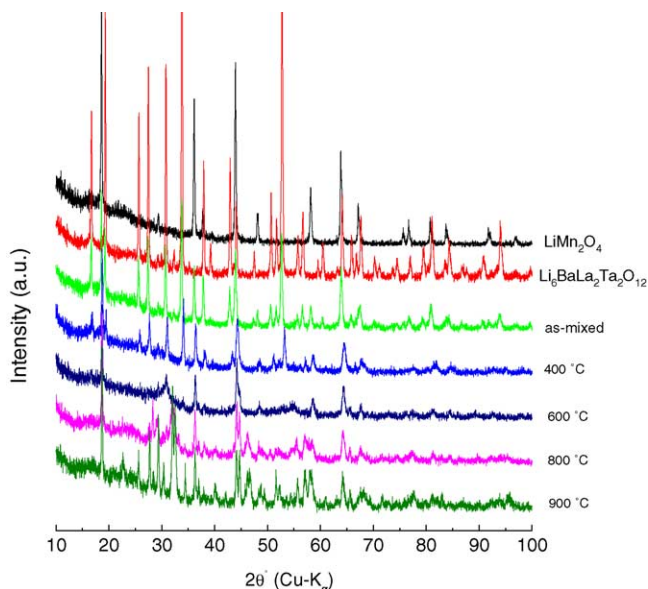


Fig. 5. Powder XRD patterns showing the reactivity between $\text{Li}_6\text{BaLa}_2\text{Ta}_2\text{O}_{12}$ and LiMn_2O_4 mixture at 400, 600, 800 and 900 °C in air. We clearly see both starting materials reflections in the 400 °C sample. At above 400 °C, the garnet-like $\text{Li}_6\text{BaLa}_2\text{Ta}_2\text{O}_{12}$ is decomposed and form reaction products. We see main reflections due to the spinel-like structure LiMn_2O_4 together with perovskite-like structure $\text{La}_2\text{LiTaO}_6$ ($2\theta \sim 23^\circ, 32^\circ$ and 45°) in the 900 °C heated sample.

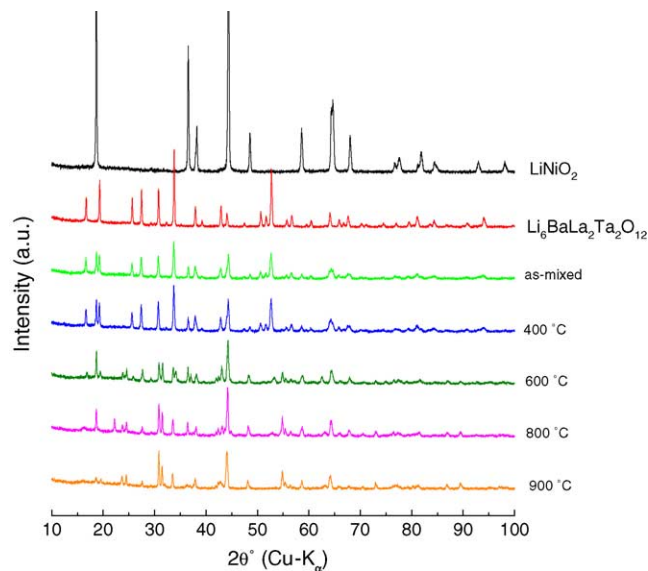


Fig. 6. Powder XRD patterns showing the reactivity between $\text{Li}_6\text{BaLa}_2\text{Ta}_2\text{O}_{12}$ and LiNiO_2 mixture at 400, 600, 800 and 900 °C in air. We clearly see both starting materials reflections in the 400 °C sample. At above 600 °C, both the garnet-like $\text{Li}_6\text{BaLa}_2\text{Ta}_2\text{O}_{12}$ and LiNiO_2 are decomposed and form reaction products.

In all other cases (Figs. 5–7), we see clearly the formation of reaction products at above 400 °C, indicating that $\text{Li}_6\text{BaLa}_2\text{Ta}_2\text{O}_{12}$ is not chemically stable against reaction with LiMn_2O_4 , LiNiO_2 and $\text{Li}_2\text{CoMn}_3\text{O}_8$ electrodes at elevated temperature. The characteristic reflections due to the

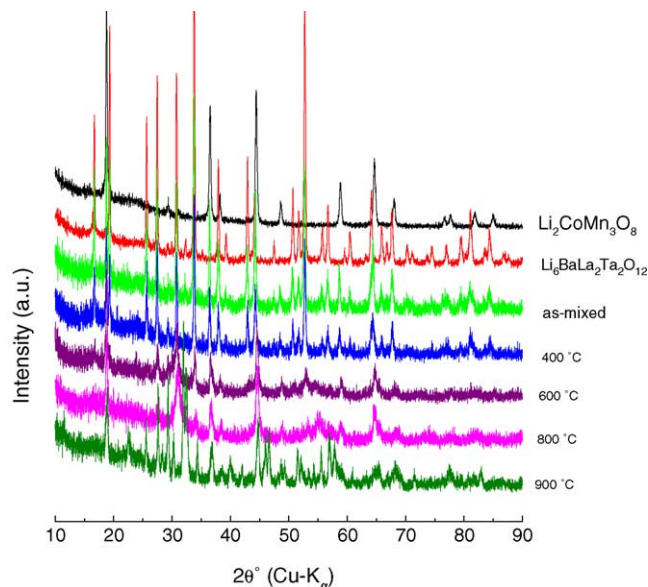
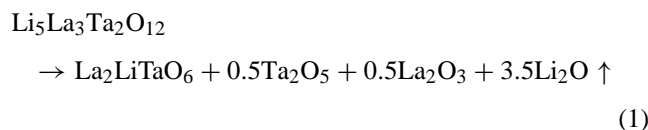


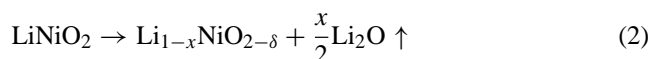
Fig. 7. Powder XRD patterns showing the reactivity between $\text{Li}_6\text{BaLa}_2\text{Ta}_2\text{O}_{12}$ and $\text{Li}_2\text{CoMn}_3\text{O}_8$ mixture at 400, 600, 800 and 900 °C in air. A similar diffraction patterns were observed for reaction mixtures of $\text{Li}_6\text{BaLa}_2\text{Ta}_2\text{O}_{12}$ with $\text{Li}_2\text{FeMn}_3\text{O}_8$. At above 400 °C, the garnet-like $\text{Li}_6\text{BaLa}_2\text{Ta}_2\text{O}_{12}$ is decomposed and form reaction products. We see clearly main reflections due to the spinel-like structure $\text{Li}_2\text{CoMn}_3\text{O}_8$ together with perovskite-like structure $\text{La}_2\text{LiTaO}_6$ ($2\theta \sim 23^\circ, 32^\circ$ and 45°) in the 900 °C heated sample.

garnet-like structure $\text{Li}_6\text{BaLa}_2\text{Ta}_2\text{O}_{12}$ phase are absent in 600, 800 and 900 °C reaction products. Typical peaks due to ordered perovskite-like structure compound $\text{La}_2\text{LiTaO}_6$ ($2\theta \sim 19^\circ, 31^\circ, 32^\circ, 37^\circ, 45^\circ$ and 56°) (JCPDS No. 39-0897) have been clearly observed (Figs. 5–7) at 800 and 900 °C together with the main peaks due to spinel-type structures LiMn_2O_4 and $\text{Li}_2\text{CoMn}_3\text{O}_8$ (Figs. 5 and 7). It appears that only a part of the electrode material is reacted with the electrolyte. A similar result was observed between $\text{Li}_6\text{BaLa}_2\text{Ta}_2\text{O}_{12}$ and $\text{Li}_2\text{FeMn}_3\text{O}_8$ mixture.

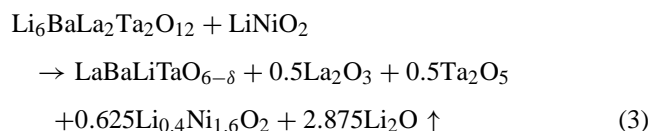
The ordered perovskite related structure compound $\text{La}_2\text{LiTaO}_6$ is thermodynamically more stable than garnet-like compound in the La–Li–Ta–O system [18]. A similar observation was made in the phase diagram investigation of three components system La_2O_3 – Li_2O – M_2O_5 ($\text{M} = \text{Nb}, \text{Ta}$) [18]. The formation of perovskite-like compound was attributed to loss of lithium oxide [18], which may be written as



It is very interesting to note that the Ba-substituted $\text{Li}_5\text{La}_3\text{Ta}_2\text{O}_{12}$ is stable against chemical reaction with LiCoO_2 up to 900 °C and up to 400 °C with the isostructural compound LiNiO_2 . LiCoO_2 appears to be thermodynamically more stable than LiNiO_2 [19,20], which is consistent with simple binary oxide stability. For example, CoO is slightly more stable ($\Delta G_f = -214 \text{ kJ mol}^{-1}$ at 25 °C) than NiO ($\Delta G_f = -211 \text{ kJ mol}^{-1}$ at 25 °C) [21]. Accordingly, LiNiO_2 decomposes into lithium deficient compounds $\text{Li}_{1-x}\text{NiO}_{2-\delta}$ ($0 < \delta < 1$), when heated at high temperature [20], according to the decomposition reaction:



Hence, LiNiO_2 may react more easily than LiCoO_2 with the garnet-like electrolyte at high temperatures. Characteristic diffraction peaks due to garnet-like structure $\text{Li}_6\text{BaLa}_2\text{Ta}_2\text{O}_{12}$ and layered structure LiNiO_2 are gradually decreases from 600 °C (Fig. 6). We see clearly the formation of ordered perovskite-like $\text{La}_2\text{LiTaO}_6$, La_2O_3 , Ta_2O_5 , and lithium deficient $\text{Li}_{1-x}\text{NiO}_{2-\delta}$ phases in the 900 °C sample (Figs. 6 and 8). Accordingly, one may propose the following chemical reaction, to explain the formation of reaction products.



It must be mentioned that $\text{Li}_6\text{ALa}_2\text{Ta}_2\text{O}_{12}$ ($\text{A} = \text{Sr}, \text{Ba}$) compounds were found to be stable against chemical reaction with molten elemental lithium [9]. From the above study, we believe that $\text{Li}_6\text{BaLa}_2\text{Ta}_2\text{O}_{12}$ could be employed as a sepa-

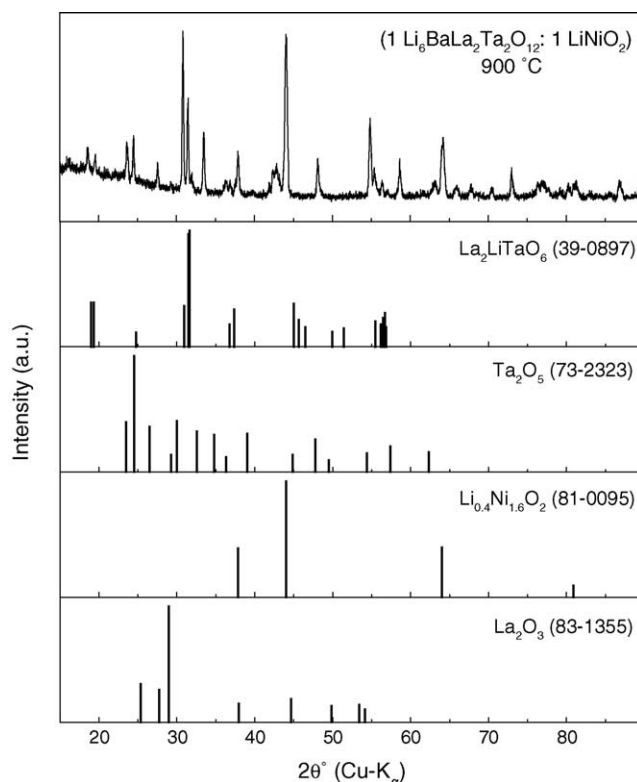


Fig. 8. Powder XRD pattern of product obtained at 900 °C for the reaction between $\text{Li}_6\text{BaLa}_2\text{Ta}_2\text{O}_{12}$ and LiNiO_2 . We see clearly diffraction peaks due to perovskite-like $\text{La}_2\text{LiTaO}_6$ (JCPDS No. 39-0897), Ta_2O_5 (JCPDS No. 73-2323), lithium deficient LiNiO_2 (JCPDS Nos. 75-0543, 81-0095) and La_2O_3 (JCPDS No. 83-1355) in the reaction product.

rator for lithium anode and LiCoO_2 cathode in the lithium battery. Further work is under progress to construct all-solid-state galvanic cells using lithium (anode), $\text{Li}_6\text{BaLa}_2\text{Ta}_2\text{O}_{12}$ (electrolyte) and LiCoO_2 (cathode).

4. Conclusions

The thick and thin $\text{Li}_6\text{BaLa}_2\text{Ta}_2\text{O}_{12}$ pellets exhibit similar lithium ion conductivity over the investigated temperature range. The chemical compatibility between $\text{Li}_6\text{BaLa}_2\text{Ta}_2\text{O}_{12}$ and several lithium battery positive electrodes (LiCoO_2 , LiMn_2O_4 , LiNiO_2 and $\text{Li}_2\text{MMn}_3\text{O}_8$ ($\text{M} = \text{Fe}, \text{Co}$)) were investigated in the temperature range 400–900 °C by powder XRD. The XRD data shows that $\text{Li}_6\text{BaLa}_2\text{Ta}_2\text{O}_{12}$ is chemically stable against reaction with 2D layered structure LiCoO_2 up to 900 °C, while other transition metal Mn, Ni, (Fe, Mn), and (Co, Mn)-based cathodes were found to react and form perovskite-like structure reaction product(s) at above 400 °C.

Acknowledgements

One of us (V.T.) thanks the Deutscher Akademischer Austauschdienst (DAAD) for financial support in the framework of guest professorship program.

References

- [1] V. Thangadurai, W. Weppner, *Ionics* 8 (2002) 281.
- [2] A.D. Robertson, A.R. West, A.G. Ritchie, *Solid State Ionics* 104 (1997) 1.
- [3] (a) X. Yu, J.B. Bates, G.E. Jellison, F.X. Hart, *J. Electrochem. Soc.* 144 (1997) 524;
(b) J.B. Bates, N.J. Dudney, B. Neudecker, A. Ueda, C.D. Evans, *Solid State Ionics* 135 (2000) 33.
- [4] H. Hyooma, K. Hayashi, *Mater. Res. Bull.* 23 (1988) 1399.
- [5] D. Mazza, *Mater. Lett.* 7 (1988) 205.
- [6] V. Thangadurai, H. Kaack, W. Weppner, *J. Am. Ceram. Soc.* 86 (2003) 437.
- [7] V. Thangadurai, S. Adams, W. Weppner, *Chem. Mater.* 16 (2004) 2998.
- [8] V. Thangadurai, W. Weppner, *J. Am. Ceram. Soc.*, in press.
- [9] V. Thangadurai, W. Weppner, *Adv. Funct. Mater.*, in press.
- [10] V. Thangadurai, W. Weppner, German Patent (Applied).
- [11] J. Schwenzel, V. Thangadurai, W. Weppner, New trends in intercalation compounds for energy storage and conversion, in: K. Zanghib, C. M. Julien, J. Prakash (Eds.), *The Electrochemical Society Proceedings, PV2003–20* 2003, Pennington, N J, USA, 2003, p. 575.
- [12] K. Kawai, M. Nagata, H. Tukamoto, A.R. West, *J. Power Sources* 81–82 (1999) 67.
- [13] JCPDS Card Nos. 48-0258; 48-0261.
- [14] V. Thangadurai, R.A. Huggins, W. Weppner, *J. Power Sources* 108 (2002) 64.
- [15] J.T.S. Irvine, D.C. Sinclair, A.R. West, *Adv. Mater.* 2 (1990) 132.
- [16] A. Manthiram, J. Kim, *Chem. Mater.* 10 (1998) 2895.
- [17] D. Linden, T.B. Reddy (Eds.), *Handbook of Batteries*, third ed., McGraw-Hill, New York, 2002.
- [18] K. Hayashi, H. Noguchi, S. Fujiwara, *Mater. Res. Bull.* 21 (1986) 289.
- [19] Y.S. Horn, S.A. Hackney, A.J. Kahaian, M.M. Thackeray, *J. Solid State Chem.* 168 (2002) 60.
- [20] H. Liu, Y.P. Wu, E. Rahm, R. Holze, H.Q. Wu, *J. Solid State Electrochem.* 8 (2004) 450.
- [21] I. Barin, *Thermodynamics data for pure substances*, VCH Publishers, New York, 1993 (Parts 1 and 2).